Passive and active neutron signatures of ^{233}U for nondestructive assay

Oskar Searfus,[1,2,*] Peter Marleau,[2] Eva Uribe,[2] Heather Reedy,[2] and Igor Jovanovic[1]

[1] *Department of Nuclear Engineering and Radiological Sciences, University of Michigan, Ann Arbor, Michigan 48109, USA*

[2] *Sandia National Laboratories, Livermore California 94550, USA*

(Received 4 October 2023; accepted 12 December 2023; published 21 December 2023)

The thorium fuel cycle is emerging as an attractive alternative to conventional nuclear fuel cycles, as it does not require the enrichment of uranium for long-term sustainability. The operating principle of this fuel cycle is the irradiation of ^{232}Th to produce ^{233}U, which is fissile and sustains the fission chain reaction. ^{233}U poses unique challenges for nuclear safeguards, as it is associated with a uniquely extreme γ-ray environment from ^{232}U contamination, which limits the feasibility of the γ-ray-based assay, as well as more conservative accountability requirements than for ^{235}U set by the International Atomic Energy Agency. Consequently, instrumentation used for safeguarding ^{235}U in traditional fuel cycles may be inapplicable. It is essential that the nondestructive signatures of ^{233}U be characterized so that nuclear safeguards can be applied to thorium fuel-cycle facilities as they come online. In this work, a set of $^{233}U_3O_8$ plates, containing 984 g^{233}U, was measured at the National Criticality Experiments Research Center. A high-pressure ^{4}He gaseous scintillation detector, which is insensitive to γ rays, was used to perform a passive fast neutron spectral signature measurement of $^{233}U_3O_8$, and was used in conjunction with a pulsed deuterium-tritium neutron generator to demonstrate the differential die-away signature of this material. Furthermore, an array of ^{3}He detectors was used in conjunction with the same neutron generator to measure the delayed neutron time profile of ^{233}U, which is unique to this nuclide. These measurements provide a benchmark for future nondestructive assay instrumentation development, and demonstrate a set of key neutron signatures to be leveraged for nuclear safeguards in the thorium fuel cycle.

DOI: 10.1103/PhysRevApplied.20.064038

I. INTRODUCTION AND BACKGROUND

Nuclear energy has long been considered a scalable, reliable candidate source of low-carbon electricity to replace fossil fuel-based power sources. In comparison to some other low-carbon sources like solar and wind, nuclear reactors can typically operate consistently independent of weather, time of day, or season. However, nuclear power is inextricably linked to the potential for nuclear proliferation, the risks of which must be mitigated. Proliferation risks are primarily mitigated by the International Atomic Energy Agency (IAEA) using nuclear safeguards as prescribed by the Treaty on the Non-Proliferation of Nuclear Weapons (NPT). Nondestructive assay (NDA) methods are well established and routinely practiced for plutonium, natural uranium (0.7% ^{235}U), and enriched uranium (>0.7% ^{235}U) in traditional light-water reactors (LWRs) and heavy-water (CANDU) fuel cycles [1,2]. However, some proposed advanced reactors and fuel cycles pose challenges to the current safeguards regime. In particular, there is a lack of NDA technology to adequately safeguard ^{233}U produced in thorium fuel cycles [3,4], compounded by the requirement that ^{233}U be accounted separately from ^{235}U when the two isotopes are colocated, since States with safeguards agreements in force with the IAEA must report quantities of ^{235}U and ^{233}U separately. [5].

A. Unique characteristics of ^{233}U in the thorium fuel cycle

Uranium-233 produced in nuclear reactors by the absorption of a neutron in ^{232}Th and the subsequent β decays of ^{233}Th and ^{233}Pa is always accompanied by trace quantities of ^{232}U, ranging from approximately 10 to 5000 ppm. This is due to several (n,2n) reactions and subsequent β decays in ^{232}Th, ^{233}Pa, and ^{233}U, which occur in the presence of fast neutrons [6]. The presence of ^{232}U is key, as its decay chain is associated with high specific activity and a high branching ratio for high-energy γ-ray emission, principally at 2.6 MeV (^{208}Tl, 35.9% branching ratio) [7]. Since ^{232}U is typically not separated from ^{233}U in thorium-based fuel cycles, this intense γ-ray environment is inextricably linked to any macroscopic quantity of ^{233}U. The activity of the 2.6-MeV γ ray, which is emitted by ^{208}Tl in 99.75% of its decays, with respect to ^{232}U concentration and time since purification is approximated

*osearfus@umich.edu

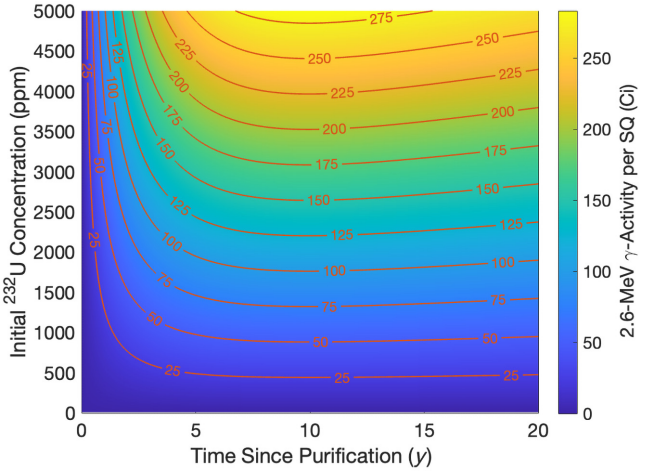

FIG. 1. Calculated activity of 2.6-MeV γ ray per one significant quantity of ^{233}U (8 kg).

by

$$A_{208}(t, C_{232}) = B_{208} C_{232} \lambda_{232} N_{233} e^{-\lambda_{232} t}[1 - e^{\lambda_{228} t}], \quad (1)$$

where C_{232} is the initial ^{232}U concentration, B_{208} is the branching ratio for production of ^{208}Tl, λ_{232} is the ^{232}U decay constant, N_{233} is the ^{233}U population, and λ_{228} is the ^{228}Th decay constant. This approximation is possible since the ^{232}U half-life (69 y) is much longer than the ^{228}Th half-life (1.9 y), and all other isotopes in the ^{232}U decay series have much shorter half-lives, on the order of seconds to days [8]. The results of this calculation are shown for a significant quantity (SQ) of ^{233}U (8 kg) [5] in Fig. 1.

B. Challenges in measurement of ^{233}U-bearing items for safeguards

Many NDA measurements of fissionable materials conducted for the purpose of nuclear safeguards involve measurement of γ-ray spectra. These measurements may quantify the total mass of some isotope, or measure the relative concentration of isotopes in thick samples. γ spectroscopy, however, is not feasible for NDA of ^{233}U items due to the intense contribution of γ rays from the ^{232}U decay chain: the intensity of the 2.6-MeV γ-ray line does not strictly correlate with the mass of ^{233}U, and γ rays directly associated with the decay of ^{233}U are low energy and low intensity and consequently not measurable above the Compton continua associated with the ^{232}U lines [4]. As an alternative, neutron-based NDA methods may be useful for safeguarding ^{233}U-bearing materials. Neutron signatures are relatively difficult to shield and generally provide more information about the bulk material as opposed to only the outer "skin" of the material, as may be the case due to self-shielding for γ-ray-based measurements. Some neutron emissions from ^{233}U-bearing materials may arise from (α,n) reactions in the material's chemical matrix, while others relate to the fissionable content of the material, either in aggregate or isotope specific.

TABLE I. Potential (α,n) reactions in ^{233}U-bearing compounds. Note that Ref. [9] gives (α,n) spectra for α radiation from ^{234}U, which is similar to that of ^{233}U.

Element	(α,n) reaction(s)	Q (MeV)	$\overline{E}_n$ for ^{234}U α [9]
O	$^{17}O + \alpha \rightarrow n + {}^{20}Ne$	0.587	2.24
	$^{18}O + \alpha \rightarrow n + {}^{21}Ne$	−0.697	
Be	$^{9}Be + \alpha \rightarrow n + {}^{12}C$	5.702	4.76
Li	$^{7}Li + \alpha \rightarrow n + {}^{10}B$	−2.790	0.33
F	$^{19}F + \alpha \rightarrow n + {}^{22}Na$	−1.952	1.24

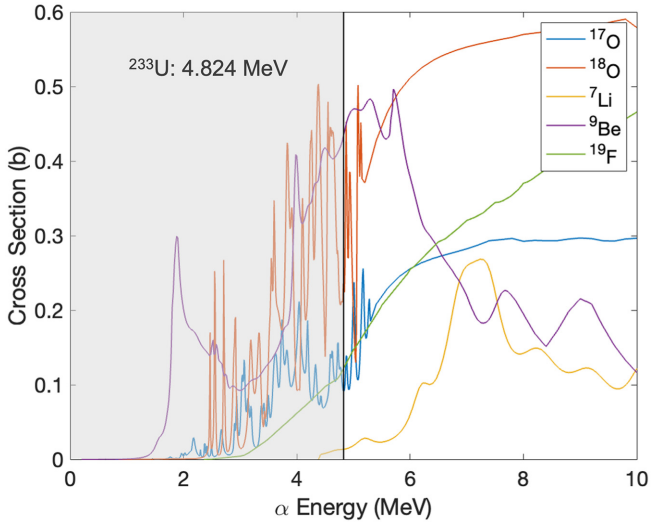

FIG. 2. (α,n) cross sections for various low-Z isotopes of interest in the thorium fuel cycle [10]. The shaded area represents possible α energies for ^{233}U, as α particles lose energy via electronic interaction before interacting with any target nucleus. b, barn.

C. Neutron signatures of ^{233}U-bearing items

1. Spontaneous neutron emission

Uranium-233-bearing objects of safeguards relevance may be in a material matrix with low-Z elements, such as oxygen (in U_3O_8 or UO_2), lithium, beryllium, or fluorine. α radiation emanating from ^{233}U can be absorbed by low-Z elements, which may then emit a neutron. These (α,n) neutrons typically have spectra that take the shape of continua up to the sum of incident α-particle energy and the Q value of the (α,n) reaction, reduced by the excitation and recoil energy of the reaction product nucleus. The reaction pathways and average neutron energies of select (α,n) sources are shown in Table I. Some (α,n) spectra contain peaks and other structures, arising from their energy-dependent cross sections, shown in Fig. 2. A major caveat to the (α,n)-based approach to ^{233}U NDA is that

the content of ^{232}U also contributes to the (α,n) signature of ^{233}U compounds: the half-life of ^{233}U (160 ky) is 2319 times longer than that of ^{232}U (69 y), so the ^{232}U α activity is significant even at ppm-scale concentrations. As a result, the α activity of ^{232}U dominates in ^{233}U samples where the ^{232}U concentration is above approximately 433 ppm. Consequently, in poor-grade (high ^{232}U content) samples, measurements based on (α,n) reactions attribute most of the neutron signal to the nonfissile ^{232}U.

The (α,n) neutrons may induce fission in ^{233}U or other fissionable species present, and thereby produce additional neutrons, with a probability determined by the multiplication of the matrix, k_{eff}. Induced fission neutrons have a distinct multiplicity and spectrum from (α,n) neutrons, so the ratio of spontaneous (α,n) to induced fission neutrons can theoretically be measured. Since this ratio is related to multiplication, it may help indicate the fissionable matrix composition.

2. Differential die-away

Pulsed differential die-away (DDA) is a technique that measures the presence of fission neutrons emitted by a target after a pulsed active interrogation source is turned off [11]. Neutrons thermalizing in the environment typically have a long lifetime compared to the duration of an active interrogation pulse, and the resultant thermal neutron population that persists beyond the fast neutron pulse has a high probability of inducing fission in fissile materials [12]. Measurement of DDA is best done with a detector, which is sensitive to fast neutrons only, as the signal-to-noise ratio (SNR) when fissile material is present is orders of magnitude higher for fast neutrons than for thermal neutrons after the pulse [13]. This technique has been previously demonstrated using cadmium-shielded ^{3}He detectors [11] and with organic scintillation detectors [12,14], the latter showing a more rapid die-away of the interrogation active background. In the case of ^{233}U and its associated γ-ray environment, however, organic scintillators may not be well suited, since the probability of pulse pile up, leading to particle misclassification, may lead to an unacceptable increase of the observed neutron background, or require extensive digital postprocessing [15].

TABLE II. Normalized delayed neutron group yields and half-lives for fast neutron-induced fission in ^{233}U and ^{235}U [24].

Isotope	Group	1	2	3	4	5	6
^{233}U	Half-life (s)	55.6	19.3	5.04	2.18	0.57	0.221
	Yield	0.095	0.208	0.242	0.327	0.087	0.041
^{235}U	Half-life (s)	54.6	20.2	5.36	2.38	0.77	0.24
	Yield	0.057	0.192	0.190	0.357	0.120	0.084

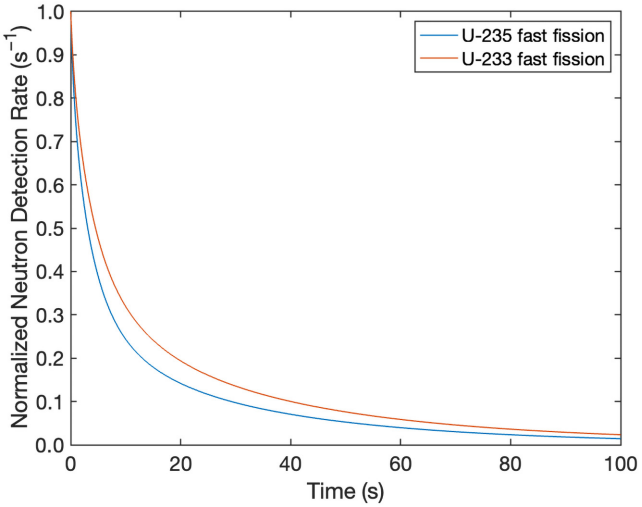

FIG. 3. Delayed neutron time profiles for fast neutron-induced fission of ^{233}U and ^{235}U, from Eq. (2) and Table II, assuming 60 s of irradiation. The neutron reaction rates are normalized to their values at $t = 0$.

3. Delayed neutron emission

When nuclei undergo fission, the resultant neutron-rich fission fragments have some probability of emitting neutrons during their radioactive decay [16–18]. This process is referred to as β-delayed neutron emission, since these neutrons are emitted in coincidence with β radiation [19]. There are many delayed neutron precursors, which are typically condensed into six groups determined by their half-lives, ranging from 0.1 to 60 s [20]. Each fissionable isotope has a unique yield for each delayed neutron group, resulting in a unique delayed neutron time profile $R(t)$ that can be modeled as

$$R(t) = B + C\sum_{i=1}^{6} Y_i[1 - e^{-t_b/\tau_i}]e^{-t/\tau_i}, \qquad (2)$$

where B is a constant background, C is a scaling factor, i is the group, Y_i is the group yield, t_b is the buildup or irradiation time, and τ_i is the group mean lifetime, which is equivalent to $t_{1/2,i}/\ln(2)$ where $t_{1/2,i}$ is the group half-life. The delayed neutron group yields for ^{233}U are shown in Table II and compared against those of ^{235}U. When fission is induced during active neutron interrogation, this time profile can be measured to indicate the isotopic composition of fissionable material [21,22], and has been shown to be resilient to common neutron shielding [23]. The delayed neutron time profiles for fast neutron-induced fission of ^{233}U and ^{235}U are shown in Fig. 3

II. METHODS

In this work, measurement of the neutron signatures of ^{233}U took place at the National Criticality Experiments

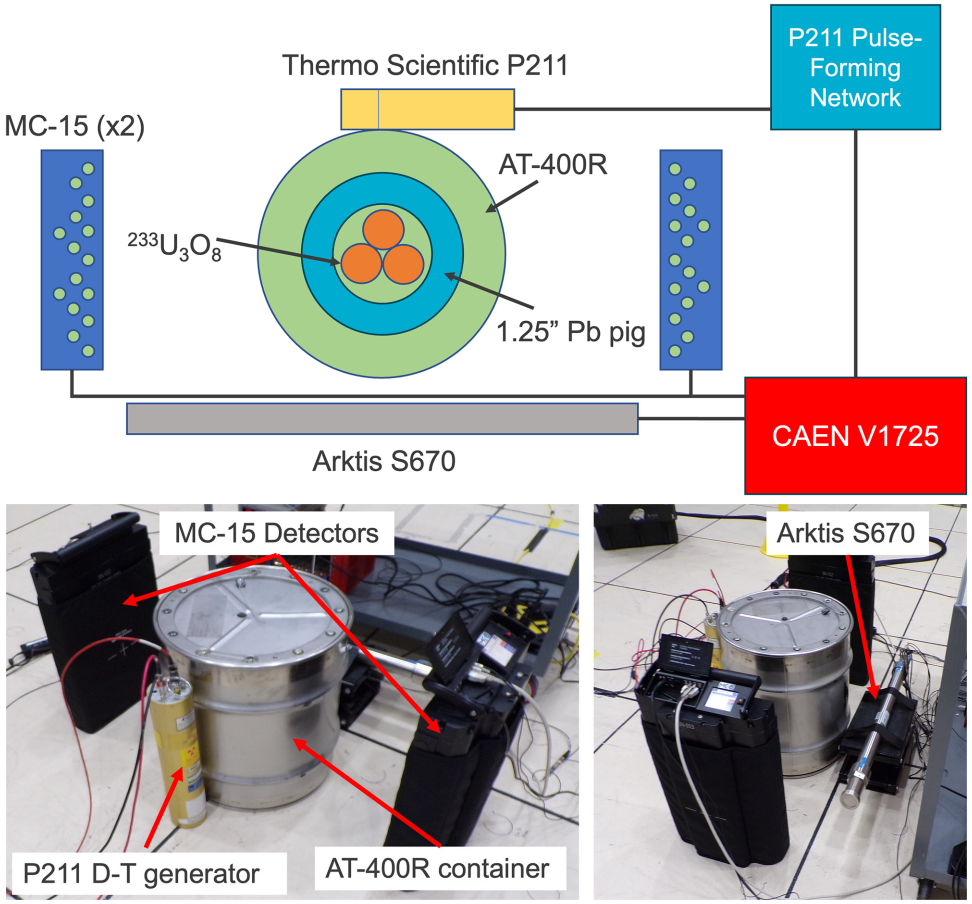

FIG. 4. Conceptual diagram illustrating the arrangement of detectors and electronics used to measure the ^{233}U plates (above). Images of the measurement setup at NCERC (below).

Research Center (NCERC), an experimental venue at the Nevada National Security Site (NSSS), which holds a variety of test objects containing nuclear materials.

A. Target and interrogation source

The material used in the experiments described in this work was a set of fuel plates fabricated for the Zero Power Reactor (ZPR) at Argonne National Laboratory. These plates comprise 33 g $^{233}U_3O_8$ powder in stainless-steel packets measuring $2 \times 3 \times 1/4$" [25]. The plates are stored in groups of 12 in steel "soup cans," three of which are stored in a triangular lattice within an AT-400R radioisotope storage container. In these measurements, the ZPR plates could not be removed from their AT-400R container, which also contains a 1.5" lead pig around the cans. Each AT-400R container holds a total of 1.188 kg $^{233}U_3O_8$, approximately 984 g of which is ^{233}U. The ^{233}U used to fabricate these ZPR plates was produced with low ^{232}U contamination, the average of which in all plates is 7 ppm. Even at this low concentration, the radiation exposure rate due to ^{232}U daughters at equilibrium in a single plate is 1000 mR/h, measured 1.5" from the center of the plate surface. Among all 36 plates, the total ^{232}U activity is approximately 157 mCi, and the corresponding ^{208}Tl activity is 56.5 mCi. At this exposure level, most γ-sensitive detectors cannot be operated due to pulse pile-up issues. In this experiment, a single AT-400R containing 36 $^{233}U_3O_8$ ZPR plates was characterized. Due to the weight of the container and its lead pig, it was placed on the concrete floor of the laboratory.

The D-T generator used as an interrogation source was a Thermo Scientific model P211. This generator has a nominal total output of 10^8 n/s, in pulses of approximately 10-μs duration, operating up to 100 Hz. This low duty cycle and high pulse intensity is advantageous for DDA analysis, as the instantaneous neutron output during pulses is high, and there is sufficient time for the neutron population to decay between pulses.

B. Neutron detectors

To detect the fast neutron signatures corresponding to passive (α,n) emissions and active interrogation DDA, an Arktis Radiation Detectors S670 [26] high-pressure ^{4}He scintillation detector was used. This detector is

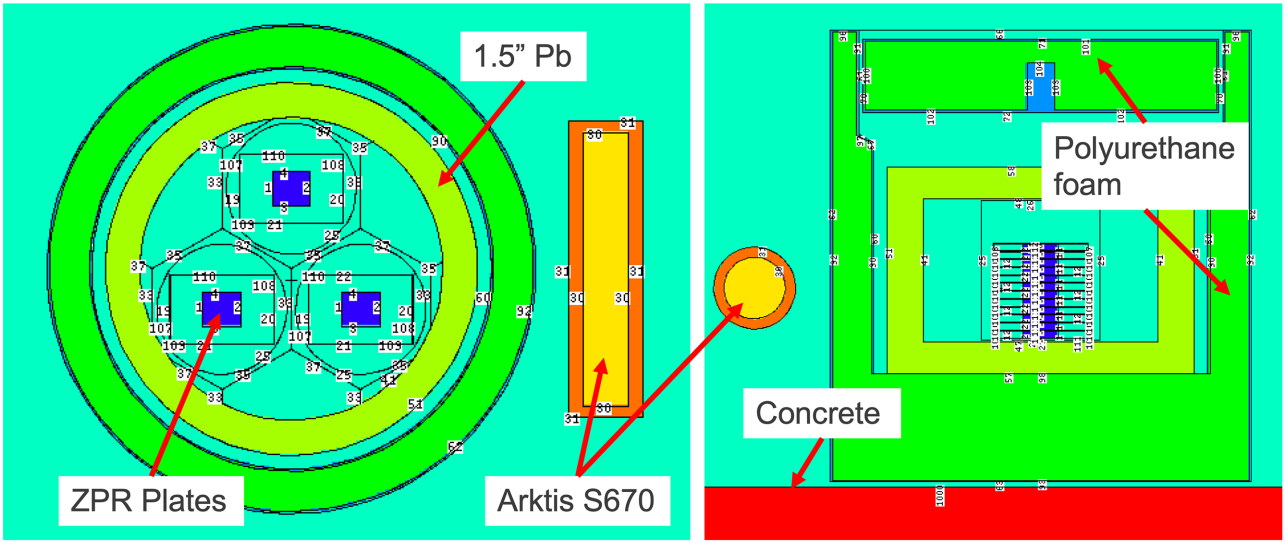

FIG. 5. MCNP geometry for simulation of DDA and DN signatures.

intrinsically sensitive to only fast neutrons if an energy deposition threshold of approximately 300 keV is used [27], measures the energy of fast neutron-induced ^{4}He recoils, and in doing so provides information on the incident neutron spectrum. This detector has a faster response time, smaller dead time, and better time resolution than most gas-based detectors based upon collection of ionization signal, since the ^{4}He scintillation pulses have a duration of approximately 1 μs. The detector and pulse analysis system applied is described in greater detail in Ref. [28].

Two MC-15 neutron multiplicity counters were also used to measure the delayed neutron time profile of the $^{233}U_3O_8$ plates. MC-15 detectors comprise an array of 15 ^{3}He proportional counters embedded in a slab of high-density polyethylene (HDPE) and are sensitive to a wide range of neutron energies [29]. They are self-contained, do not require any external electronics to function, and provide a logic (TTL) pulse output for each neutron detection event. These detectors are efficient in detecting neutrons in the energy range of delayed neutrons (approximately 0.001 to 2 MeV [19]), but because they must thermalize neutrons before detecting them, their time resolution is poor compared to the S670 detector. Consequently, MC-15 detectors were used to measure the time profile of delayed neutrons, but not DDA. The measurement configuration, showing the target material, interrogation source, and detectors are shown in Fig. 4.

C. Electronics and experimental operation

A CAEN V1725 14-bit, 250 MS/s digitizer and CAEN CoMPASS 2.0 software [30] were used to collect waveforms from the S670 and MC-15 detectors. The P211 D-T generator has analog control, and was configured to run at 100 Hz for 6000 pulses. A trigger out logic signal from the P211 pulse-forming network, approximately 10 μs prior to neutron production, was also digitized. To measure the DDA time profile, the time period between events in the S670 detector and the most recent logic signal from the pulse-forming network were considered (i.e., between pulses), whereas for the delayed neutron time profile, the time period between events in the MC-15 detectors and the 6000th logic signal were considered (i.e., after the D-T generator was turned off). While the P211 settings ideally correspond to a total irradiation period of 60 s, it was observed that the actual pulse frequency of the generator was approximately 107 Hz, corresponding to an actual irradiation period of 56 s.

The passive fast neutron emission signature of the $^{233}U_3O_8$ plates was measured using the S670 detector for a total period of 1200 s, and also provided the passive background for measurement of the DDA signature. To measure DDA and delayed neutron emission, 40 irradiation cycles were carried out. The irradiation cycle period was 300 s, of which 56 s corresponds to pulsed irradiation to build up the delayed neutron precursor population and measure the DDA signature, and the remainder corresponds to D-T generator off time, which allows for measurement of the delayed neutron time profile. An additional 10 irradiation cycles were performed with the AT-400R container removed, to serve as an active background for the DDA measurement. The analysis shown in this work represents the data from all irradiation cycles in aggregate.

D. Monte Carlo simulation

The DDA and DN signatures of the $^{233}U_3O_8$ plates were simulated using MCNPX-PoliMi [31,32]. The geometry of the AT-400R container, shielding, and its contained ZPR plates is based on Refs. [33,34] and is shown in Fig. 5. The P211 D-T generator was approximated as a monoenergetic

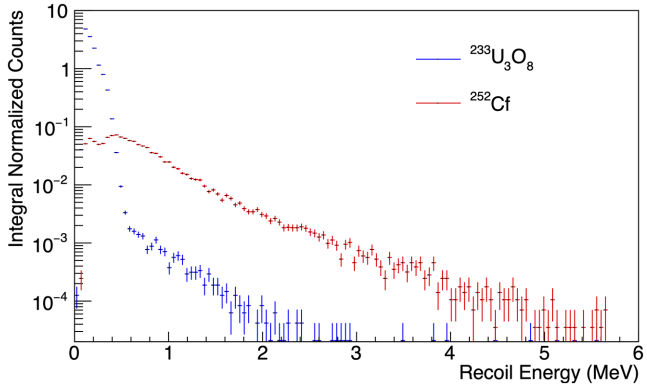

FIG. 6. Passive fast neutron spectral signature of $^{233}U_3O_8$ measured with the S670 ^{4}He detector, compared to the measured spectrum of ^{252}Cf. The spectra are normalized to their integral above 300-keV energy deposition, above which there are no contributions from γ radiation.

14.1-MeV isotropic point source. In postprocessing, the temporal behavior of the neutron source was approximated by adding time randomly sampled from a 10-μs-wide uniform distribution to each history in the PoliMi collisional output file. To simulate the delayed neutron time profile, neutron emissions from the ^{233}U plates that occur more than 10 ms after the D-T generator pulse were recorded, since delayed neutron emissions occur on such a long time scale that their time signature is immune to radiation transport-induced time-distortion effects. To approximate the effect of the D-T generator irradiation period, time randomly sampled from a 56-s-wide uniform distribution was added to the delayed neutron histories.

III. RESULTS

A. Passive signatures

The passive spectrum of $^{233}U_3O_8$ is shown in Fig. 6 and compared against a ^{252}Cf spontaneous fission neutron

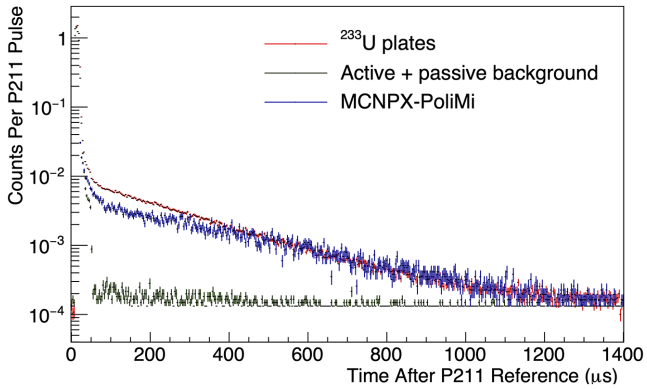

FIG. 7. DDA measurement of ZPR plates with the S670 ^{4}He detector, compared against background and simulation.

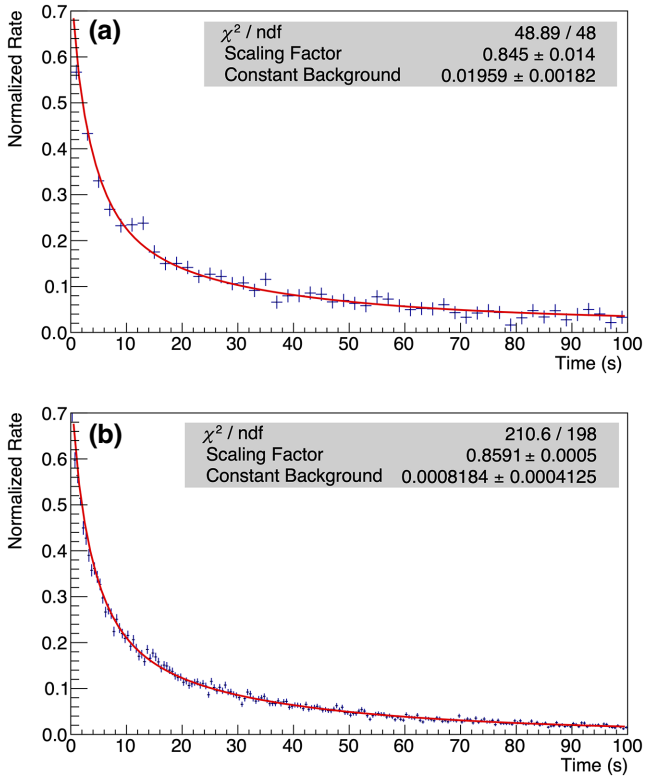

FIG. 8. Delayed neutron decay measurement of ZPR plates as measured with MC-15 detectors (above) and simulated with MCNPX-PoliMi (below). Time profiles are normalized to the sum of the first 4 s. The measured time profile has 2-s-wide bins, while the simulated time profile has 0.5-s-wide bins. Fits to Eq. (2) and Table II are shown in red.

source, as measured with the S670 ^{4}He detector. The neutron source emanating from the $^{233}U_3O_8$ plates exhibits a characteristically lower-energy endpoint when compared to the ^{252}Cf fission source, as is expected from ^{17,18}O(α,n) reactions. The intensity of this ^{233}U O(α,n) spectrum is proportional to ^{233}U mass at low concentrations of ^{232}U and at low multiplication, and is consequently a potential candidate for NDA of ^{233}U under these circumstances.

B. Differential die-away

The DDA microscopic time profile of the ZPR plates measured with the S670 ^{4}He detector is shown in Fig. 7 and compared against the sum of active and passive backgrounds. Only pulses corresponding to at least 300-keV recoil energy deposition were accepted in generating DDA time profiles, for both measurement and simulation. The fission neutron signal remained visible above background for about 1200 μs after the generator pulse, in agreement with simulation. The measured DDA time profile shows a clear exponential decay significantly above the background, implying that DDA measured with this detector

TABLE III. Results of fitting delayed neutron data in this work to various fissionable isotope delayed neutron parameters. Parameters for ^{233}U and ^{235}U from Ref. [24], for ^{238}U from Ref. [35], for ^{239}Pu from Ref. [36], and for ^{232}Th from Ref. [37].

Isotope	Dataset	C	B	χ^2/ndf
^{233}U	Measured	0.8450 ± 0.0140	0.0196 ± 0.0018	48.9 / 48
^{235}U		0.9146 ± 0.0172	0.0249 ± 0.0021	58.6 / 48
^{238}U		1.454 ± 0.080	0.0008 ± 0.2615	547 / 48
^{239}Pu		0.9288 ± 0.0046	0.025 ± 0.002	65.3 / 48
^{232}Th		1.012 ± 0.005	0.0306 ± 0.0018	96.0 / 48
^{233}U	MCNPX-PoliMi	0.8591 ± 0.0005	0.00082 ± 0.00041	211 / 198
^{235}U		0.9202 ± 0.0007	0.0064 ± 0.0004	294 / 198
^{238}U		1.152 ± 0.007	0.0138 ± 0.0003	936 / 198
^{239}Pu		0.9369 ± 0.0064	0.0062 ± 0.0003	369 / 198
^{232}Th		1.031 ± 0.009	0.0109 ± 0.0006	777 / 198

may be a strong candidate for confirmation of the presence of ^{233}U. At low multiplication, the fast neutron DDA signal intensity is proportional to fissile mass, so this technique may be used for quantification of total fissile content in the presence of ^{233}U, in the case that the measurement and neutron moderation geometries are tightly constrained.

C. Delayed neutrons

The delayed neutron time profile of ^{233}U measured with the MC-15 detectors is shown in Fig. 8, and compared to the simulated time profile. The time profiles are fit to Eq. (2), with tabular delayed neutron yields and half-lives for ^{233}U for 14.1-MeV neutrons given in Table II. The only fitting parameters used are the scaling factor C and the flat constant background B. To demonstrate the uniqueness of these fits to delayed neutrons from ^{233}U specifically, the fit results when the time profiles are forced to fit delayed neutron yield parameters for other fissionable isotopes are shown in Table III. Both the measured and simulated time profiles are best fit by the delayed neutron parameters for ^{233}U, however, the distinction is clearer in the simulated time profile, likely due to its superior statistics and lack of passive background.

IV. CONCLUSIONS AND FUTURE WORK

In this work, three signatures of ^{233}U were investigated for their feasibility in future NDA methods for international safeguards of thorium fuel cycles: passive fast neutron spectroscopy, differential die-away analysis, and delayed neutron time-profile analysis. An experiment was performed to measure these signatures at NCERC, using nearly a kilogram of ^{233}U in the form of $^{233}U_3O_8$, representing the largest-scale NDA measurement of ^{233}U to date.

The fast neutron spectral signature of $^{233}U_3O_8$ is shown to be readily measurable with the γ-insensitive S670 ^{4}He detector, and clearly differentiable from a generic spontaneous fission neutron source. Consequently, this technique could be well suited to discriminating between oxides of ^{233}U and plutonium, for example.

Measurement of the fast neutron DDA time profile of ^{233}U was also demonstrated with the S670 detector and a pulsed D-T neutron generator for the first time, indicating a potentially unique capability of the ^{4}He scintillation detector.

The delayed neutron time profile of ^{233}U, induced using the same D-T neutron generator, was measured using an array of moderated ^{3}He proportional counters. The measured time profile showed a good fit to the time profile generated from nuclear data, and matched the simulated time profile. Delayed neutron time profiles are isotope specific, so their measurement may allow for discrimination between and separate quantification of ^{233}U and ^{235}U, which is one of the primary challenges in NDA for safeguarding thorium fuel cycles. In future work, delayed neutron-based techniques should be further investigated with mixed-isotope (^{233}U and ^{235}U) items, so that separate isotope quantification can be demonstrated.

ACKNOWLEDGMENTS

The authors would like to thank J. Walker and J. Hutchinson of Los Alamos National Laboratory for their help in coordinating the experiment at NCERC. The work of O. Searfus was performed under appointment to the Nuclear Nonproliferation International Safeguards Fellowship Program sponsored by the National Nuclear Security Administration's Office of International Nuclear Safeguards (NA-241). Sandia National Laboratories is a multimission laboratory managed and operated by National Technology Engineering Solutions of Sandia, LLC, a wholly owned subsidiary of Honeywell International Inc., for the U.S. Department of Energy's National Nuclear Security Administration under Contract No. DE-NA0003525. This work was funded in part by the Consortium for Monitoring, Technology, and Verification under the Department of Energy National Nuclear Security

Administration Award No. DE-NA0003920. The National Criticality Experiments Research Center is supported by the DOE Nuclear Criticality Safety Program, funded and managed by the National Nuclear Security Administration.

[1] D. Reilly, N. Ensslin, H. J. Smith, and S. Kreiner, *Passive nondestructive assay of nuclear materials* (1991).

[2] *Safeguards Techniques and Equipment:*, International Nuclear Verification Series No. 1 (Rev. 2) (International Atomic Energy Agency, Vienna, 2011).

[3] L. G. Worrall, A. Worrall, G. F. Flanagan, S. Croft, A. M. Krichinsky, C. A. Pickett, R. D. M. Jr., S. L. Cleveland, D. N. Kovacic, J. M. Whitaker, and J. L. White-Horton, Safeguards considerations for thorium fuel cycles, Nucl. Technol. **194**, 281 (2016).

[4] L. G. Worrall, V. Henzl, A. Swift, N. Luciano, E. Cervi, J. Cooley, B. Davies, J. S. Denton, A. Favalli, B. Grogan, A. Krichinsky, K. Hogue, M. L. Lockhart, D. J. Mercer, A. Milojevich, J. Stinnett, R. Reed, and A. Worrall, *Safeguards Technology for Thorium Fuel Cycles: Research and Development Needs Assessment and Recommendations*, Tech. Rep. (Oak Ridge National Laboratory, 2021).

[5] *IAEA Safeguards Glossary*, International Nuclear Verification Series No. 3 (International Atomic Energy Agency, Vienna, 2022).

[6] U. E. Humphrey and M. U. Khandaker, Viability of thorium-based nuclear fuel cycle for the next generation nuclear reactor: Issues and prospects, Renewable Sustainable Energy Rev. **97**, 259 (2018).

[7] R. Gehrke, V. Novick, and J. Baker, γ-ray emission probabilities for the ^{232}U decay chain, Int. J. Appl. Radiat. Isot. **35**, 581 (1984).

[8] J. Turner, *Atoms, Radiation, and Radiation Protection* (Wiley, New York, NY, 2008).

[9] G. N. Vlaskin and Y. S. Khomyakov, (α, n) neutron spectra on thick light targets, At. Energy **130**, 104 (2021).

[10] T. Murata, H. Matsunobu, and K. Shibata, *Evaluation of the (α, xn) reaction data for JENDL/AN-2005*, Tech. Rep. JAEA-Research–2006-052 (Japan, 2006).

[11] D. L. Chichester and E. H. Seabury, in *2008 IEEE Nuclear Science Symposium Conference Record* (IEEE, Dresden, Germany, 2008), p. 3361.

[12] C. A. Miller, W. A. Peters, F. Y. Odeh, T. H. Shin, M. Mamtimin, S. D. Clarke, T. L. Grimm, and S. A. Pozzi, Subcritical assembly die-away analysis with organic scintillators, Nucl. Instrum. Methods Phys. Res., Sect. A: Accelerators, Spectrometers, Detectors and Associated Equipment **959**, 163598 (2020).

[13] R. C. Runkle, D. L. Chichester, and S. J. Thompson, Rattling nucleons: New developments in active interrogation of special nuclear material, Nucl. Instrum. Methods Phys. Res., Sect. A: Accelerators, Spectrometers, Detectors and Associated Equipment **663**, 75 (2012).

[14] M. C. Hamel, J. K. Polack, M. L. Ruch, M. J. Marcath, S. D. Clarke, and S. A. Pozzi, Active neutron and gamma-ray imaging of highly enriched uranium for treaty verification, Sci. Rep. **7**, 7997 (2017).

[15] X. Luo *et al.*, Pulse pile-up identification and reconstruction for liquid scintillator based neutron detectors, Nucl. Instrum. Methods Phys. Res., Sect. A: Accelerators, Spectrometers, Detectors and Associated Equipment **897**, 59 (2018).

[16] R. B. Roberts, L. R. Hafstad, R. C. Meyer, and P. Wang, The delayed neutron emission which accompanies fission of uranium and thorium, Phys. Rev. **55**, 664 (1939).

[17] R. B. Roberts, R. C. Meyer, and P. Wang, Further observations on the splitting of uranium and thorium, Phys. Rev. **55**, 510 (1939).

[18] D. J. Hughes, J. Dabbs, A. Cahn, and D. Hall, Delayed neutrons from fission of u^{235}, Phys. Rev. **73**, 111 (1948).

[19] P. Dimitriou *et al.*, Development of a reference database for beta-delayed neutron emission, Nucl. Data Sheets **173**, 144 (2021), special Issue on Nuclear Reaction Data.

[20] G. R. Keepin, T. F. Wimett, and R. K. Zeigler, Delayed neutrons from fissionable isotopes of uranium, plutonium, and thorium, Phys. Rev. **107**, 1044 (1957).

[21] J. Nattress, K. Ogren, A. Foster, A. Meddeb, Z. Ounaies, and I. Jovanovic, Discriminating uranium isotopes using the time-emission profiles of long-lived delayed neutrons, Phys. Rev. Appl. **10**, 024049 (2018).

[22] K. Ogren, J. Nattress, and I. Jovanovic, Discriminating uranium isotopes based on fission signatures induced by delayed neutrons, Phys. Rev. Appl. **14**, 014033 (2020).

[23] K. Ogren, T. Wu, J. Nattress, and I. Jovanovic, The effects of low-z shielding on uranium isotope discrimination using the time-emission profiles of long-lived delayed neutrons, Nucl. Instrum. Methods Phys. Res., Sect. A: Accelerators, Spectrometers, Detectors and Associated Equipment **1019**, 165847 (2021).

[24] L. V. East, R. H. Augustson, H. O. Menlove, and C. F. Masters, Delayed-neutron abundances and half-lives from 14.7-MeV fission, Trans. Amer. Nucl. Soc. **13**: 760–1 (1970).

[25] R. G. Nicol, J. R. Parrott, A. M. Krichinsky, W. D. Box, C. W. Martin, and W. R. Whitson, *Fabrication of Zero Power Reactor Fuel Elements Containing U-233*, Tech. Rep. (Oak Ridge National Laboratory, 1982).

[26] *S670: Fast Neutron Detector*, Arktis Radiation Detectors Ltd., Zurich, Switzerland (2022).

[27] O. Searfus, C. Meert, S. Clarke, S. Pozzi, and I. Jovanovic, in *2022 IEEE Nuclear Science Symposium* (IEEE, Milan, Italy, 2022).

[28] O. Searfus, K. Ogren, and I. Jovanovic, Digital pulse analysis for fast neutron recoil spectroscopy with a ^{4}He scintillation detector, Nucl. Instrum. Methods Phys. Res., Sect. A: Accelerators, Spectrometers, Detectors and Associated Equipment **1046**, 167703 (2023).

[29] C. E. Moss, M. A. Nelson, R. B. Rothrock, and E. B. Sorensen, *MC-15 Users Manual* (2018).

[30] *CoMPASS: Multiparametric DAQ Software for Physics Applications*, CAEN S.p.A., Viareggio, Italy (2022).

[31] D. B. Pelowitz, *MCNPX User's Manual: Version 2.7.0*, Tech. Rep. LA-CP-11-00438 (Los Alamos National Laboratory, 2011).

[32] S. Pozzi, S. Clarke, W. Walsh, E. Miller, J. Dolan, M. Flaska, B. Wieger, A. Enqvist, E. Padovani, J. Mattingly, D. Chichester, and P. Peerani, MCNPX-PoliMi for nuclear nonproliferation applications, Nucl. Instrum.

Methods Phys. Res., Sect. A: Accelerators, Spectrometers, Detectors and Associated Equipment **694**, 119 (2012).

[33] R. E. Glass, *AT-400R Affirmation Summary*, Tech. Rep. SAND98-1231/1 (Sandia National Laboratories, 1996).

[34] K. N. Schwinkendorf, *Criticality Safety Index Determination for ORNL 233U ZPR Fuels in AT-400R Containers*, Tech. Rep. NCSE-CSID-2011-001 (National Security Technologies LLC, 2011).

[35] V. M. Piksaikin, V. A. Roshchenko, and G. G. Korolev, Relative yield of delayed neutrons and half-life of their precursor nuclei from ^{238}U fission by 14.2–17.9 MeV neutrons, At. Energy **102**, 151 (2007).

[36] V. Roshchenko, V. Piksaikin, L. Kazakov, and G. Korolev, Relative yield of delayed neutrons and half-life of their precursor nuclei with fissioning of ^{239}PU by 14.2–17.9 MeV neutrons, At. Energy **101**, 897 (2006).

[37] V. A. Roshchenko, V. M. Piksaikin, G. G. Korolev, and A. S. Egorov, Time features of delayed neutrons and partial emissive-fission cross sections for the neutron-induced fission of ^{232}Th nuclei in the energy range 3.2–17.9 MeV, Phys. At. Nucl. **73**, 913 (2010).